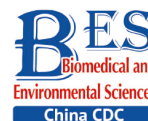


Letter to the Editor

**Pulmonary Nodules Developed Rapidly in Staffs in the Isolation Ward of a Chinese Hospital during the COVID-19 Epidemic***

LI Yu Hua^{1,&}, YU Ke Wen^{2,&}, SUN Neng Jun³, JIN Xiao Dong⁴, LUO Xin¹,
YANG Jing⁵, HE Bing^{1,#}, and LI Bo^{6,#}

In December 2019, the novel 2019 coronavirus disease (COVID-19) emerged in Wuhan and spread all over the country. The Zibo Central Hospital had set up a febrile clinic and isolation ward for confirmed and suspected patients since January 23, 2020. Suspected patients were hospitalized immediately to the isolation ward. Every healthcare staff was authorized to undergo low-dose computed tomography (LDCT) of the chest free of charge before and after their assignment in the isolation ward. If suspected lesions were found on the second computed tomography (CT), polymerase chain reaction (PCR) and nucleic acid tests were carried out. Isolation was finished 2 weeks later if all examination results remained normal. During this period, we found that the number of pulmonary nodules markedly increased in the second CT in most of the healthcare staff, so we performed a retrospective analysis of the second chest CT images in 46 healthcare workers (subjects). The prevalence, characteristics, size, density, and distribution of pulmonary nodules on the second CT were analyzed. We attempt to reveal this phenomenon and call attention to the harm that an isolation environment can contribute to health care workers and help establish treatment for pulmonary nodules scientifically and rationally.

This study was approved by the Institutional Ethics Committee for Human Subjects of Zibo Central Hospital, China. All study procedures were performed in accordance with the Fleischner Society guidelines. Although the hospital had a free policy, in consideration of radiation exposure, only 46 staff

members had two LDCT examinations. All staff members were healthy and remained healthy during the observation period.

All chest CT examinations were performed using Toshiba Aquilion ONE. The imaging parameters were as follows: 120 Kvp, 30 mA, rotation time of 0.5 s, and pitch of 0.98. The slice thickness of reconstructed images was 1 mm. All subjects were examined by computer-aided diagnosis and artificial screening. CAD was set to display nodules with a diameter of more than 1 mm. Artificial screening was performed by three radiologists using a standard lung window [center, 500 Hounsfield units (HU); width, 1,500 HU]. For each pulmonary nodule, the longest axial diameter (mm), CT value (HU), and shortest distance from the pleural surface (mm) were recorded. SPSS 25.0 software (IBM Corp., Armonk, NY, USA) was used for statistical analysis.

In this study, a total of 46 subjects were enrolled, including 27 (58.69%) with pulmonary nodule and 19 (41.31%) without nodule in the first CT. The second CT showed 16 (34.78%) subjects without nodules, 30 (65.22%) with nodules, 20 (43.48%) with new-onset nodules (Table 1). Compared with the first CT, the average number of nodules in the second CT increased from 1.46 ± 1.75 to 2.62 ± 3.18 in the ≤ 35 -year-old group ($n = 26$, $P = 0.002$) and increased from 1.75 ± 1.83 to 4.35 ± 6.37 in the > 35 -year-old group ($P = 0.047$) (Supplementary Figure S1A available in www.besjournal.com). The average number of pulmonary nodules increased from 1.89 ± 1.81 to

doi: 10.3967/bes2020.127

*This study was supported by the Natural Science Foundation of China [No. 81700321] and the Key Research and Development Plan of Shandong Province [2018GSF118140].

1. Department of Imaging, Shandong University Central Hospital of Zibo, Zibo 255036, Shandong, China; 2. Department of internal medicine, Maternal and Child Health Hospital of Zibo, Zibo 255000, Shandong, China; 3. Department of medical administration, Shandong University Central Hospital of Zibo, Zibo 255036, Shandong, China; 4. Department of Geriatrics, Shandong University Central Hospital of Zibo, Zibo 255036, Shandong, China; 5. Binzhou Medical University, Yantai 264003, Shandong, China; 6. Department of Cardiology, Shandong University Zibo Central Hospital, Zibo 255000, Shandong, China

4.67 ± 6.54 in 18 male subjects ($P = 0.049$) and increased from 1.39 ± 1.75 to 2.54 ± 3.21 in 28 female subjects ($P = 0.006$) (Supplementary Figure S1B available in www.besjournal.com). As revealed by some studies, pathogenic factors of pulmonary nodules were age, environment, autoimmunity, toxic gas damage, infection, tumor history, etc.^[1-3]. Once a suspected patient was confirmed to have COVID-19, he or she would be transferred immediately to Shandong Province Chest Hospital by a special vehicle. Because confirmed patients stay in the isolation ward for only a short time, under strict isolation and

disinfection measures, the probability of COVID-19 infection was small, and PCR and nucleic acid test results were normal. After multiple laboratory examinations, these subjects were found to have no signs of respiratory virus infection. Except for two subjects with smoking history, none of the subjects had the abovementioned factors. We hypothesized that new-onset nodules may be related to the use of disinfectants containing chlorine.

As shown in the first CT, 69 nodules (95%) had diameter of < 6 mm, 4 nodules (5%) had diameter of 6–8 mm, but there was no nodule with diameter of

Table 1. Characteristics and prevalence of pulmonary nodules in the health care staff

Characteristics	First CT ($n = 46$)		Second CT ($n = 46$)		
	Subjects without nodules n (%)	Subjects with nodules n (%)	Subjects without nodules n (%)	Subjects with nodules n (%)	Subjects with new-onset nodules n (%)
Mean age	33.667 ± 1.777	35.704 ± 0.965	33.933 ± 1.876	35.156 ± 0.976	35.450 ± 1.184
Gender (male)	4 (21.05)	14 (51.85)	4 (25)	14 (46.67)	10 (50)
Patients and nodules	19 (41.31)	27 (58.69)	16 (34.78)	30 (65.22)	20 (43.48)
History of tumor	0	0	0	0	0
History of smoking	0	2 (4.35)	0	2 (4.35)	2 (4.35)
Classification of nodule					
Solid nodules		46 (63.01)		62 (40)	16 (19.51)
Subsolid nodules		2 (2.74)		40 (25.81)	38 (46.34)
Ground glass nodules		11 (15.07)		39 (25.16)	28 (34.15)
Calcified nodules		14 (19.18)		14 (9.03)	0
Longest axial diameter					
< 6 mm		69 (94.52)		151 (97.42)	82 (100)
6–8 mm		4 (5.48)		4 (2.58)	0
> 8 mm		0		0	0
Location					
Right upper lobe		18 (24.66)		34 (21.93)	15 (18.30)
Right middle lobe		8 (10.96)		22 (14.19)	10 (12.20)
Right lower lobe		15 (20.55)		35 (22.58)	22 (26.82)
Left upper lobe		14 (19.17)		27 (17.42)	14 (17.07)
Left lower lobe		18 (24.66)		37 (23.87)	21 (25.61)
Distance from the pleura					
< 5 mm		24 (32.87)		62 (40.00)	38 (46.34)
5–10 mm		16 (21.92)		40 (25.81)	24 (29.27)
10–15 mm		12 (16.44)		21 (13.55)	9 (10.97)
15–20 mm		9 (12.33)		13 (8.38)	4 (4.88)
> 20 mm		12 (16.44)		19 (12.26)	7 (8.54)
Total nodules		73		155	82

> 8 mm. In the second CT, 151 nodules (97%) had diameter of ≤ 6 mm, 4 nodules (5%) had diameter of 6–8 mm, but there was no nodule with diameter of > 8 mm (Supplementary Figure S2A available in www.besjournal.com). Paired *t*-test showed a significant increase in the average numbers of nodules with diameter of ≤ 6 mm (1.50 ± 1.70 vs. 3.28 ± 4.75 , $P = 0.004$) (Supplementary Figure S2B available in www.besjournal.com). The results demonstrated that all new-onset nodules were small. The 2017 Fleischner Society guidelines indicated that pulmonary nodules with diameter of < 6 mm do need not annual follow-up (4). The guidelines have no treatment guidance for short-term new-onset pulmonary nodules. We suggested that health care workers should not be anxious but pay attention to the occurrence of fever, cough, and other respiratory symptoms.

The distribution of new-onset nodules was as follows: 15 nodules in the right upper lobe, 10 nodules in the right middle lobe, 22 nodules in the right lower lobe, 14 nodules in the left upper lobe, and 21 nodules in the left lower lobe (Supplementary Figure S3A available in www.besjournal.com). Compared with the first CT, the average number of nodules in all lobes have increased significantly in the second CT: right upper lobe, 0.39 ± 0.68 vs. 0.74 ± 1.10 ($P = 0.022$); right middle lobe, 0.17 ± 0.38 vs. 0.48 ± 0.89 ($P = 0.009$); right lower lobe, 0.33 ± 0.60 vs. 0.76 ± 1.45 ($P = 0.020$), left upper lobe, 0.30 ± 0.66 vs. 0.59 ± 1.02 ($P = 0.011$), and left lower lobe, 0.39 ± 0.64 vs. 0.80 ± 1.07 ($P = 0.002$) (Supplementary Figure S3B available in www.besjournal.com).

According to Fleischner Society guidelines, the pulmonary nodules were divided into four categories: solid nodules, subsolid nodules, ground glass nodules, and calcified nodules^[4,5]. The first CT showed 46 (63%) solid nodules, 2 (3%) subsolid nodules, 11 (15%) ground glass nodules, and 14 (19%) calcified nodules (Figure 1A). The second CT detected 62 (40%) solid nodules, 40 (26%) subsolid nodules, 39 (25%) ground glass nodules, and 14 (9%) calcified nodules (Figure 1A). New-onset nodules included 16 (20%) solid nodules, 38 (46%) subsolid nodules, and 28 (34%) ground glass nodules (Figure 1A). Compared with the first CT, densities of nodules increased in varying degrees in the second CT: solid nodules, 1.00 ± 1.40 vs. 1.35 ± 1.64 ($P = 0.019$); subsolid nodules, 0.04 ± 0.21 vs. 0.87 ± 2.78 ($P = 0.049$); ground glass nodules, 0.24 ± 0.67 vs. 0.83 ± 1.43 ($P = 0.002$); and calcified nodules, 0.30 ± 0.63 vs. 0.30 ± 0.63 (Figure 1B).

The shortest distances to the pleural surface in the first CT scan were as follows: 24 nodules, < 5 mm; 16 nodules, 5–10 mm; 12 nodules, 10–15 mm; 10 nodules, 15–20 mm; and 12 nodules, > 20 mm (Supplementary Figure S4A available in www.besjournal.com). In the second CT, shortest distances to the pleural surface were as follows: 48 nodules, < 5 mm; 34 nodules, 5–10 mm; 19 nodules, 10–15 mm; 12 nodules, 15–20 mm; and 18 nodules, > 20 mm (Supplementary Figure S4A). The shortest distances for the new-onset nodules were as follows: 37 nodules, < 5 mm, 24 nodules, 5–10 mm; 9 nodules, 10–15 mm; 4 nodules, 15–20 mm; and 7 nodules, > 20 mm (Supplementary Figure S4A). Compared with the first CT, the distances of the pulmonary nodules to the pleura increased in different degrees in the second CT: 0–5 mm, 0.52 ± 0.91 vs. 1.35 ± 2.41 ($P = 0.004$); 5–10 mm, 0.35 ± 0.74 vs. 0.87 ± 1.60 ($P = 0.014$), 10–15 mm, 0.26 ± 0.53 vs. 0.46 ± 0.69 ($P = 0.011$); 15–20 mm, 0.20 ± 0.45 vs. 0.28 ± 0.58 ($P = 0.103$); and > 20 mm, 0.26 ± 0.49 vs. 0.41 ± 0.69 ($P = 0.018$) (Supplementary Figure S4B available in www.besjournal.com).

During the COVID-19 epidemic, strict disinfection was carried out frequently. The floor of the isolation ward was disinfected four times a day using a disinfectant containing 500–1,000 mg/L of chlorine. Although the ward has regulated ventilation, some subjects said that the pungent smell of chlorine lingered in the air. It could be speculated that the chlorine content in the air in the isolation ward was higher than that in ordinary wards. Exposure of both humans and animals to chlorine causes lung injury, and chlorine was more likely to damage the alveolar^[6]. Chlorine could induce various injuries (alveolar injury or airway injury) depending on the inhalation dose and concentration^[7]. To our knowledge, no study has presented similar results, especially on the effect of long-term inhalation of small chlorine doses on human lungs. Previous studies have highlighted the potential importance of the maintenance of mitochondrial function in the recovery of the chlorine-damaged lung^[8]. Differences in autoimmunity might explain why not all subjects had new-onset pulmonary nodules. With this immune regulatory mechanism, a mild lung injury caused by chlorine inhalation might heal itself^[9]. In this study, one subject had undergone third CT at 1.5 months after the second CT, which revealed that most of the new-onset nodules disappeared (Figure 2) without therapy.

In conclusion, the number of pulmonary nodules

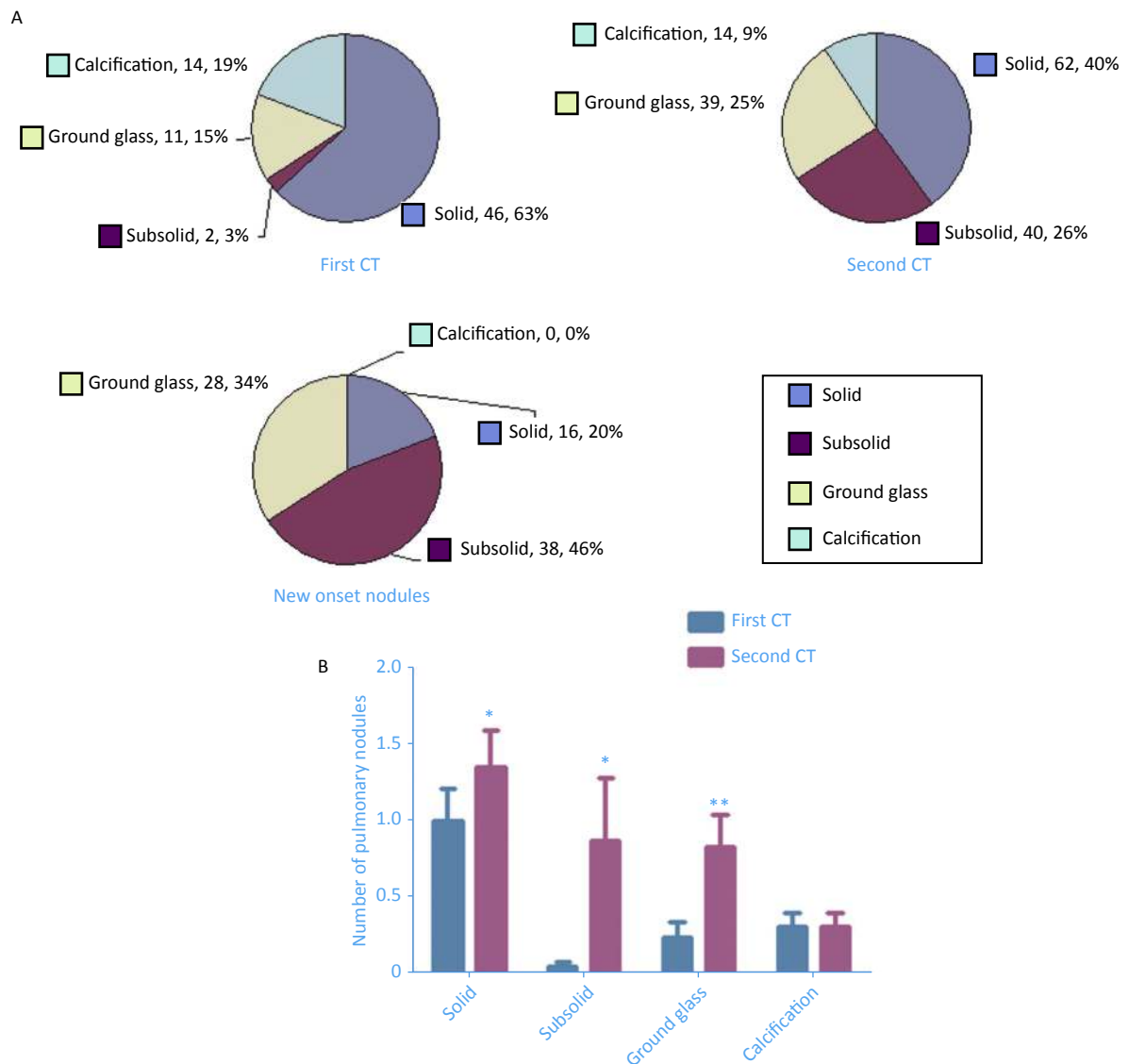


Figure 1. Number of pulmonary nodules of different densities detected in the first computed tomography (CT) and second CT as well as new-onset nodules (A). Paired *t*-test shows increases in the average number of nodules with different densities: solid nodules ($P = 0.019$), subsolid nodules ($P = 0.049$), ground glass nodules ($P = 0.002$), and calcified nodules (B).

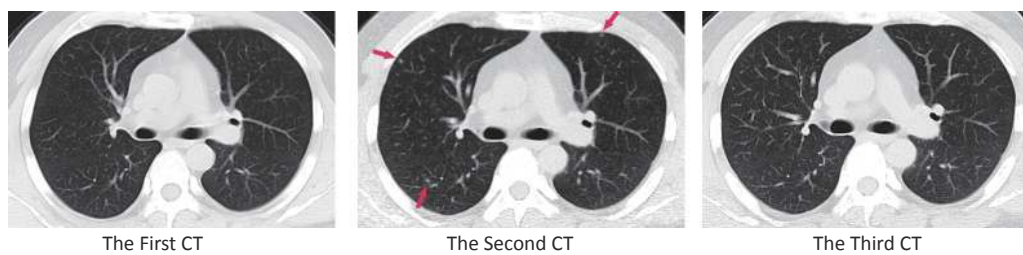


Figure 2. Compared with the first computed tomography (CT), the second CT showed three new-onset pulmonary nodules: a 3-mm solid nodule in the anterior segment of the upper lobe of the right lung, a 3-mm subsolid nodule in the dorsal segment of the lower lobe of the right lung, and a 2-mm subsolid nodule in the anterior lobe of the left superior lobe. The nodules disappeared in the third CT.

increased in part-time staff members who was on duty in the isolation ward. Most of the new-onset nodules were subsolid and ground glass nodules and distributed near the pleura. Annual follow-up was recommended. The environment of the isolation ward disinfected with chlorine-containing disinfectant may be harmful to the respiratory system of health care staff. Hospitals should pay attention to the respiratory protection of its staff. We also recommended establishing criteria on chlorine concentration in the air of a working environment.

No potential conflicts of interest were disclosed.

LI Bo and HE Bing designed this paper; LI Bo also did all the statistical work. LI Yu Hua and YU Ke Wen collected data and wrote the manuscript. LUO Xin, LI Yu Hua, and HE Bing collected imaging data. SUN Neng Jun, YANG Jing, and JIN Xiao Dong were involved in part in the study design and data collection. All authors reviewed the manuscript.

[&]These authors contributed equally to this work.

[#]Correspondence should be addressed to LI Bo, Tel: 86-18560292371, E-mail: libosubmit@163.com; HE Bing, Tel: 86-13505330797, E-mail: heb613003@126.com

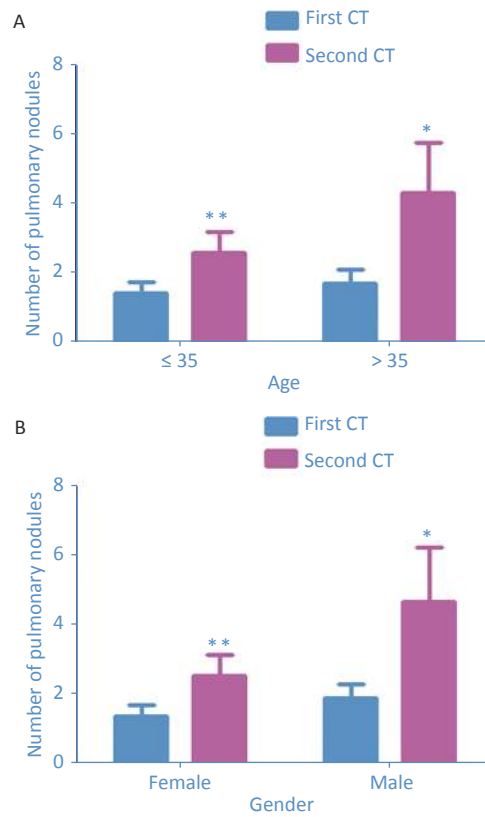
Biographical notes of the first authors: LI Yu Hua, female, born in 1977, MM, majoring in the imaging diagnosis of respiratory system disease; YU Ke Wen, male, born in 1971, BM, majoring in the diagnosis and treatment of respiratory system disease.

Received: August 8, 2020;

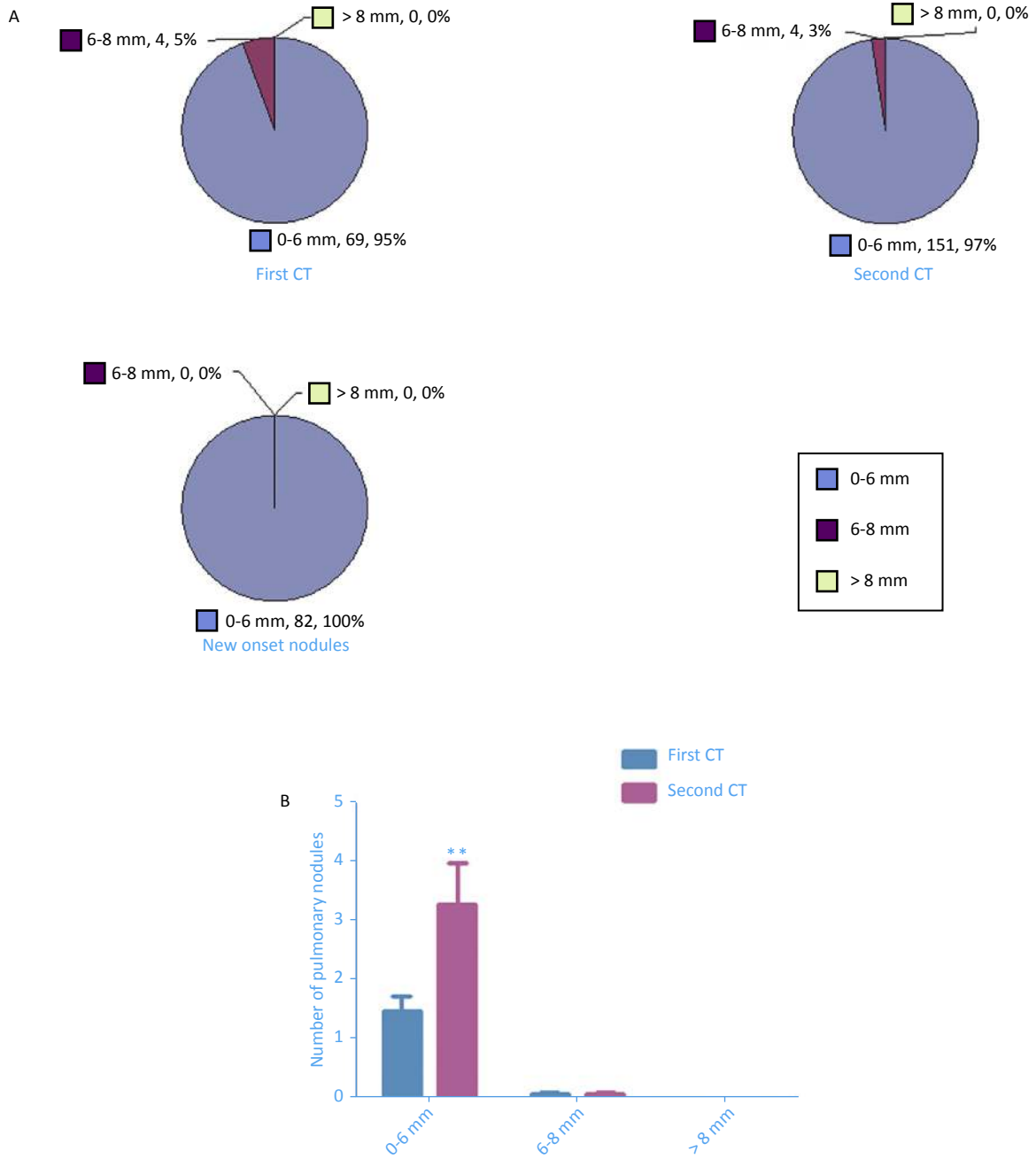
Accepted: November 15, 2020

REFERENCES

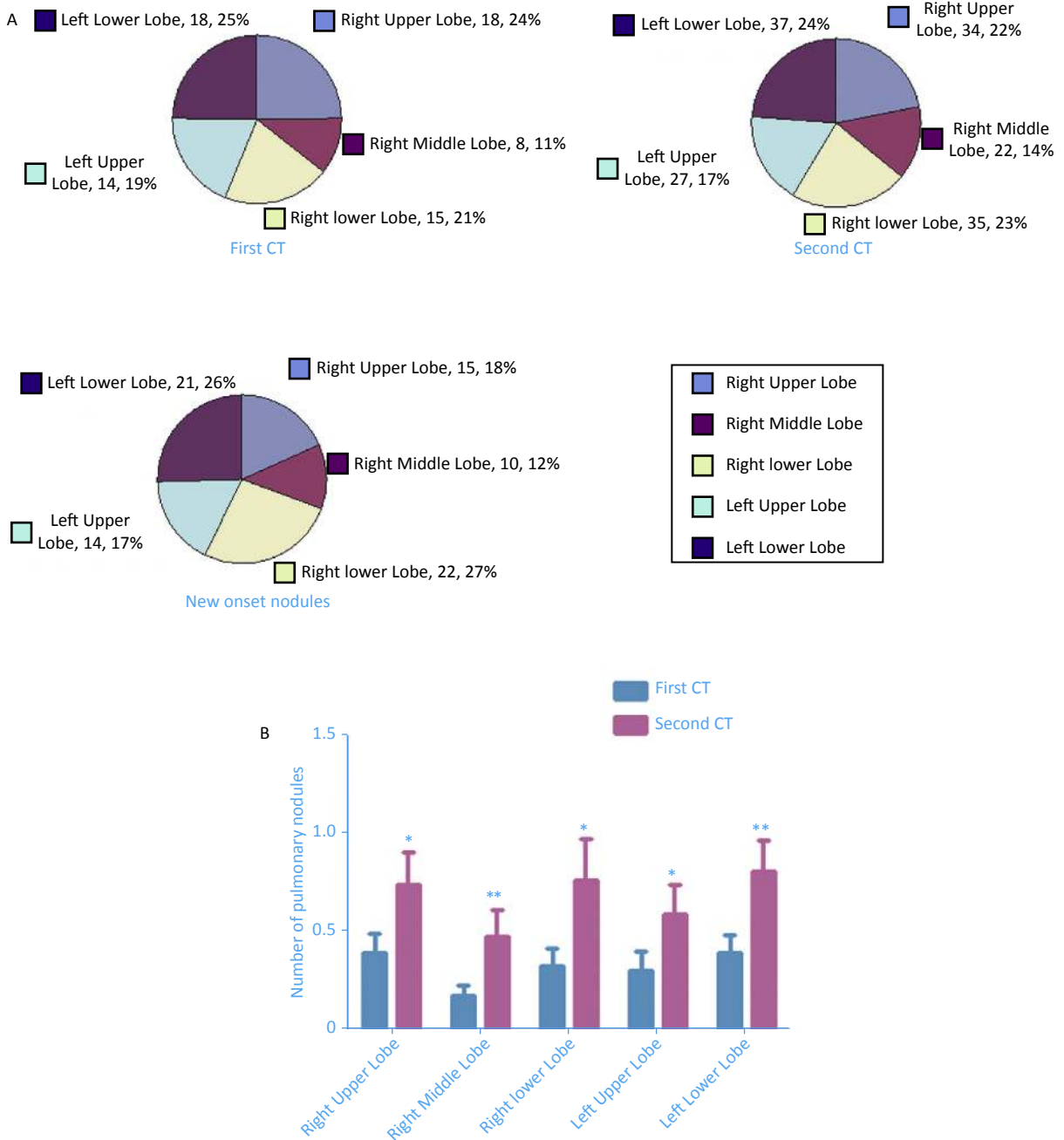
1. Murphy D, Sinha–Royle E, Bellis K, et al. Nodular rheumatoid arthritis (RA): A distinct disease subtype, initiated by cadmium inhalation inducing pulmonary nodule formation and subsequent RA-associated autoantibody generation. *Med Hypotheses*, 2019; 122, 48–55.
2. He YT, Zhang YC, Shi GF, et al. Risk factors for pulmonary nodules in North China: a prospective cohort study. *Lung Cancer*, 2018; 120, 122–9.
3. Ergün R, Evcik E, Ergün D, et al. High-resolution computed tomography and pulmonary function findings of occupational arsenic exposure in workers. *Balkan Med J*, 2017; 34, 263–8.
4. MacMahon H, Naidich DP, Goo JM, et al. Guidelines for management of incidental pulmonary nodules detected on CT images: from the Fleischner Society 2017. *Radiology*, 2017; 284, 228–43.
5. MacMahon H, Austin JHM, Gamsu G, et al. Guidelines for management of small pulmonary nodules detected on CT scans: a statement from the Fleischner Society. *Radiology*, 2005; 237, 395–400.
6. Bracher A, Doran SF, Squadrito GL, et al. Targeted aerosolized delivery of ascorbate in the lungs of chlorine-exposed rats. *J Aerosol Med Pulm Drug Deliv*, 2012; 25, 333–41.
7. Li WL, Pauluhn J. Phosgene-induced acute lung injury (ALI): differences from chlorine-induced ALI and attempts to translate toxicology to clinical medicine. *Clin Transl Med*, 2017; 6, 19.
8. Jurkuvenaite A, Benavides GA, Komarova S, et al. Upregulation of autophagy decreases chlorine-induced mitochondrial injury and lung inflammation. *Free Radic Biol Med*, 2015; 85, 83–94.
9. Yadav AK, Bracher A, Doran SF, et al. Mechanisms and modification of chlorine-induced lung injury in animals. *Proc Am Thorac Soc*, 2010; 7, 278–83.



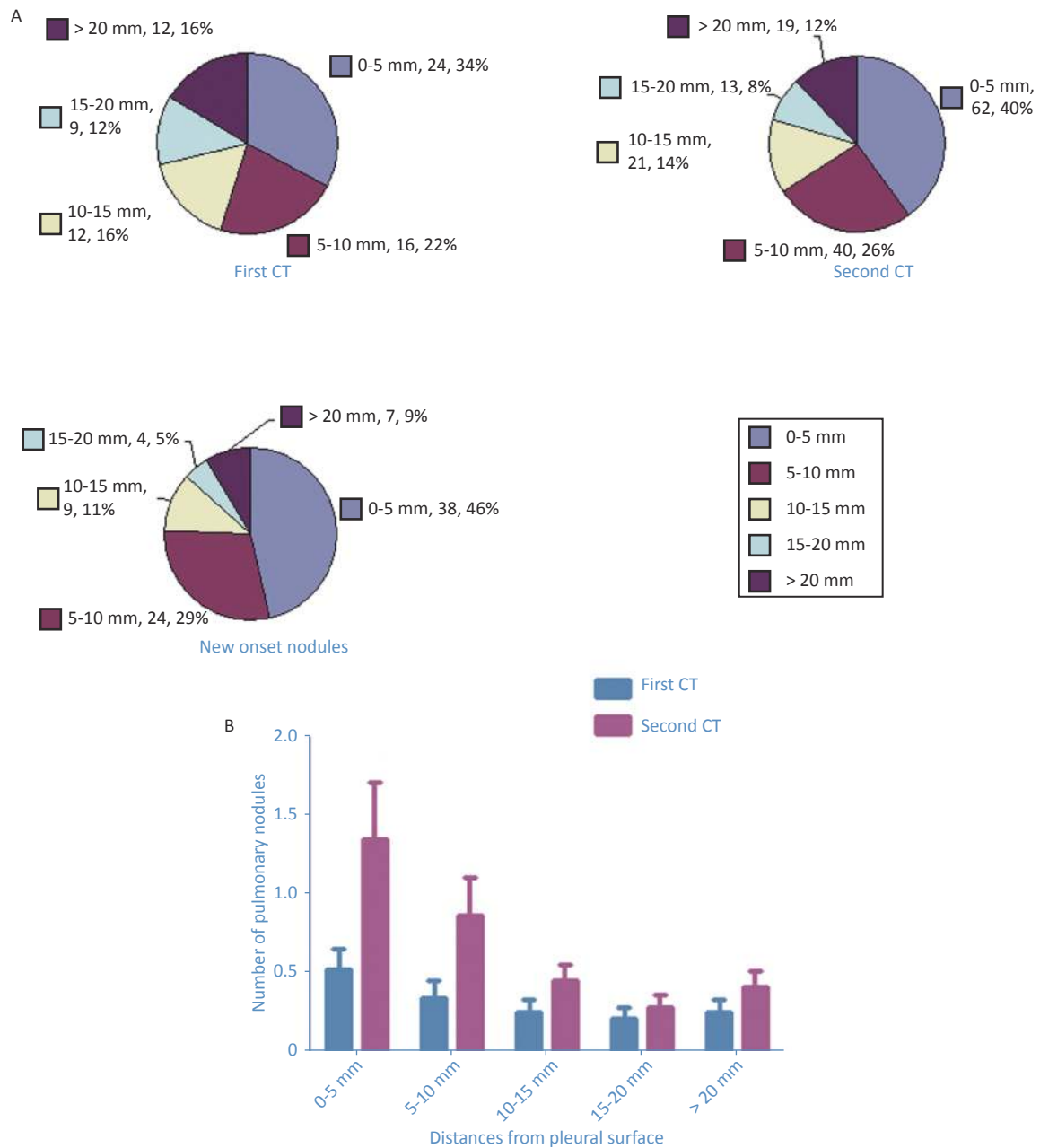
Supplementary Figure S1. Comparison of the increase of the number of pulmonary nodules according to age and gender from the two CT scans. The number of pulmonary nodules increased significantly in all groups of age ≤ 35 -year old group ($n = 26$, $P = 0.002$), > 35 -year old group ($n = 20$, $P = 0.047$), the males ($n = 18$, $P = 0.049$), and the females ($n = 28$, $P = 0.006$) (A and B).



Supplementary Figure S2. Pie chart showed the number of pulmonary nodules detected in the first CT scan, the second CT scan, as well as the new onset nodules (A). The number of pulmonary nodules increased significantly in all sizes of ≤ 6 mm, 6–8 mm, and > 8 mm. Paired *t* test showed significant increases of averaged numbers of nodules ≤ 6 mm ($P = 0.004$), with no change in nodules 6-8 mm and > 8 mm (B).



Supplementary Figure S3. Pie chart showed the number of pulmonary nodules detected in each pulmonary lobe in the first CT scan, the second CT scan, as well as the new onset nodules (A). Paired t test showed significant increases of averaged numbers of nodules in each pulmonary lobe: right upper lobe ($P = 0.022$), right middle lobe ($P = 0.009$), right lower lobe ($P = 0.020$), left upper lobe ($P = 0.011$), and left lower lobe ($P = 0.002$) (B).



Supplementary Figure S4. Pie chart showed the number of pulmonary nodules of different distances from the pleural surface detected in the first CT scan, the second CT scan, as well as the new onset nodules (A). Paired t test showed the increases of averaged numbers of nodules of different distances from the pleural surface: 0–5 mm ($P = 0.004$), 5–10 mm ($P = 0.014$), 10–15 mm ($P = 0.011$), 15–20 mm ($P = 0.103$), and > 20 mm ($P = 0.018$) (B).